607

Nanoapertures for AFM-based single-molecule force spectroscopy

Stephan F. Heucke

Center for Nanoscience and Department of Physics,
Ludwig-Maximilians-Universität München,
Amalienstr. 54, 80799 Munich, Germany
Email: stephan.heucke@lmu.de

Elias M. Puchner

Department of Cellular and Molecular Pharmacology,
University of California,
600 – 16th Street, San Francisco, CA 94158, USA
Email: elias.puchner@ucsf.edu

Stefan W. Stahl

Center for Nanoscience and Department of Physics,
Ludwig-Maximilians-Universität München,
Amalienstr. 54, 80799 Munich, Germany
Email: stefan.stahl@physik.uni-muenchen.de

Alexander W. Holleitner

Walter Schottky Institut and Physik-Department,
Technische Universität München,
Am Coulombwall 4a, 85748 Garching, Germany
Email: holleitner@wsi.tum.de

Hermann E. Gaub*

Center for Nanoscience and Department of Physics,
Ludwig-Maximilians-Universität München,
Amalienstr. 54, 80799 Munich, Germany
Email: gaub@lmu.de
*Corresponding author

Philip Tinnefeld

Physikalische und Theoretische Chemie – NanoBioSciences,
Technische Universität Braunschweig,
Hans-Sommer-Strasse 10, 38106 Braunschweig, Germany
Email: p.tinnefeld@tu-braunschweig.de

Abstract: Simultaneous single-molecule force spectroscopy and microfluorescence binding measurements are often hampered by background fluorescence from the bulk. Zero-Mode Waveguides (ZMW) restrict the excited volume but require a special design, which allows the tip of the force probing cantilever to protrude into the nanoaperture. Here, we describe the design and fabrication of such ZMW and report the first experiments where binding of fluorescent adenosine triphosphate to the force-activated enzyme titin kinase was measured while the enzyme was subjected to mechanical forces.

Biographical notes: Stephan F. Heucke received his MSc in Physics from St Andrews University, Scotland, in 2007. He is currently finalising his PhD in Physics at LMU. His research interests include nanopositioning, manipulation and fluorescence spectroscopy of single molecules, metallic nanostructures and force spectroscopy of biomolecules.

Elias M. Puchner studied Physics at the LMU Munich and received his PhD from Hermann Gaub's Lab. He combined AFM-based single-molecule force spectroscopy and fluorescence microscopy to study mechanoenzymatic processes and to assemble biomolecules to complexes. In his current postdoctoral research in the Lim Lab at UCSF, he investigates the spatial organisation and regulation of signalling proteins in cells.

Stefan W. Stahl studied Physics at the LMU Munich and graduated in 2008. He received his PhD at the chair of Hermann Gaub at the LMU Munich in August 2012. His research interests include AFM-based single-molecule force spectroscopy experiments and its combination with fluorescent techniques.

Alexander W. Holleitner currently is an Associate Professor at TU Munich. He studied Physics at LMU Munich where he received his PhD in 2002. He then went to UCSB for postdoctoral research. His interests lie in optical and electronic phenomena on the nanometre scale, methods of nanostructuring and physical characterisation of solid-state devices.

Hermann E. Gaub studied Physics in Ulm and received his PhD form the TU-Munich before going to Stanford for postdoctoral research. He currently holds the chair in Applied Physics at the LMU-Munich. He pioneered the use of atomic force microscopy for the study of the mechanical properties of single molecules.

Philip Tinnefeld studied Chemistry in Münster, Montpellier and Heidelberg. In 2002, he received his PhD from the University of Heidelberg. After his Habilitation at the University of Bielefeld, he became Professor at LMU-Munich. Since 2010 he is Professor of Biophysical Chemistry at TU Braunschweig. His research interests include the development of microscopy techniques and applications of DNA nanotechnology to study problems at the interface of physics, chemistry and biology.

1   Introduction

The rapidly evolving single-molecule techniques have revolutionised modern life sciences. Since the first realisation of this concept in single-ion channel recordings, the access to properties of individuals rather than the collective response of an ensemble has brought stunning insight into a broad range of phenomena and opened entire new research fields [1]. For example, fluorescence microscopy with single-molecule resolution allows imaging beyond the Abbe limit or in combination with Förster Resonance Energy Transfer (FRET) the relative localisation of labels with angstrom precision [2]. Mechanical experiments with single-molecule resolution and piconewton sensitivity provided for the first time control over a new and, as it turned out, extremely important parameter in molecular interaction: force [3]. The functional mechanisms of molecular motors were interrogated with techniques like AFM and optical tweezers, and forces governing protein folding or nucleic acid suprastructures were determined [4–7].

With its superb position control with sub-Å precision, the AFM moreover provides an additional feature, which goes far beyond force spectroscopy. It allows the molecular manipulation of individual molecules at surfaces. With the introduction of Single-Molecule Cut & Paste (SMC&P), a technique became available which allows for a controlled pick up of individual molecules, like proteins from a surface, and their one by one deposition at a chosen position at a surface [8].

It is obvious that a combination of these two strong single-molecule techniques, fluorescence and mechanics, provides a realm of new possibilities of controlled manipulation. Hybrid instruments were developed that allowed in one-half space of the sample the manipulation of the molecules by AFM and in the other half fluorescence microscopy in TIRF excitation via the microscope objective [9]. New phenomena such as force-triggered enzyme reactions were investigated, or the functional reconstitution of individual RNA aptamers by SMC&P was monitored [10, 11].

In previous studies, we had investigated by AFM-based single-molecule force spectroscopy the force-activation of titin kinase (TK), a functional module in the giant muscle protein titin, which organises the molecular architecture of the sarcomere and provides its passive elasticity [12–14]. We had shown that the auto-inhibition of this enzyme is removed by a stretching force of 40 pN exposing the putative active site [12]. A direct observation of the binding of adenosine triphosphate (ATP) for example by means of fluorescence would unambiguously clarify this process. To design such a simultaneous single-molecule optomechanical experiment and to elucidate the boundary conditions for such an investigation was the motivation of this study.

When the mechanically probed molecules are labelled either covalently or via a high affinity binder and where no fluorescent molecules remain in the sample volume the experimental designs are straightforward. However in cases where a limited affinity of the label results in substantial background fluorescence from the bulk fluorophores, discrimination of the single molecule under investigation against the background soon

becomes a limiting problem. Particularly for the investigation of interactions of soluble ligands in equilibrium with an immobilised receptor at the surface, the background signal of ligands in solution may overwhelm the single-molecule signal from the surface.

The contribution of the bulk molecules to the signal may be estimated as follows: both in Confocal Fluorescence Microscopy (CFM) and TIRF excitation, the detection volume has a lower bound of somewhat less than $1\ \mu m^3$. Background fluorescence caused by the labels of mobile ligands in this volume will come from

$$n = cVN_A \qquad\qquad\qquad (1)$$

molecules where c is the ligands' molar concentration, V is the detection volume and N_A is Avogadro's number. This means that for a signal-to-background ratio of 1 and a minimum voxel volume of $1\ \mu m^3$ the concentration of analytes in solution must not exceed a concentration of 0.16 nM.

In order to study interactions amongst molecules close to equilibrium, the interaction partners need to be present in concentrations on the order of the equilibrium constant. Particularly when enzymes are to be studied in their interaction with labelled substrates, this boundary condition imposes severe limitations, particularly at high Michaelis–Menten constants. Figure 1 depicts a histogram of all Michaelis–Menten constants for enzymes known today. It is an updated version of the viewgraph that Samiee et al. [15] used to rationalise the need for improved methods to reduce background fluorescence. It shows that the large majority of enzymes known to date have a K_M around 100 μM and can therefore not be investigated with conventional fluorescence microscopy techniques, like CFM or TIRFM.

Figure 1   Histogram of Michaelis–Menten constants (K_M) for 62,000 enzymes taken from the Brenda database (see http://www.brenda-enzymes.info). It emphasises how conventional fluorescence techniques fail to observe single-enzyme kinetics at natural concentrations of labelled substrates. The use of Zero-Mode Waveguides (ZMW), however, allows experiments at label concentrations up to 100 μM (see online version for colours)
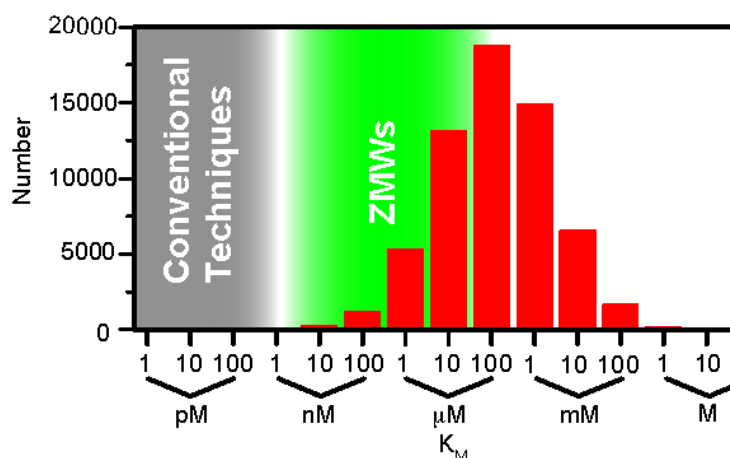
Due to the nature of our proposed experiment, there is generally another reason to work near equilibrium than its obvious physiological relevance: the time window in which an enzyme that is subject to an activating force is able to form an enzyme-substrate complex

is usually limited, as the current force-pulling techniques will not be able to prevent rupture for arbitrarily long times. Thus, low-affinity ligand must be compensated with high-substrate concentration.

The labs of Web and Craighead found a very elegant means to reduce the background fluorescence. They used nanoapertures in metal films which they called Zero-Mode Waveguides (ZMW) and measured the emission of fluorophores form within the holes [16]. Since the largest part of the voxel is occupied by metal, only the remaining aperture volume may contribute to the bulk background signal. An additional reduction of the excitation volume comes from the field geometry within the nanoaperture. Since ZMWs have diameters much smaller than the wavelength of the incident light that they allow zero light propagation. Instead, the incoming light gets reflected at the apertures and an evanescent field illuminates only at the bottom of the waveguides.

Since their introduction in 2003 by Levene et al., ZMWs have proven their applicability in a variety of studies: besides relatively straightforward fluorescence correlation spectroscopy of protein–protein interactions [17], diffusion within lipid bilayers inside ZMWs [18] could be monitored as well as membrane regions of living cells [19]. Most prominently, the use of ZMWs in a massively parallel approach allowed time- and cost-efficient DNA-sequencing [20].

In the present work, we will first describe the fabrication of ZMWs by Focused-Ion-Beam (FIB) milling. We then characterise their design and discuss handling and storage issues that have to be dealt with when using ZMWs. We will show fluorescence spectroscopy data form within our ZMWs and introduce the experiments combining force and fluorescence spectroscopy in a set-up schematically depicted in Figure 2. Finally, we will present initial results of ATP binding to titin kinase in ZMWs and discuss what further improvements are to be done to standardise force spectroscopy in ZMWs.

Figure 2 Schematic diagram of the conducted experiment: an AFM cantilever triggers the enzymatic activity of a force-regulated enzyme immobilised at the bottom of a zero-mode waveguide. Additionally to the force–distance information from the AFM, the binding of fluorescently labelled substrates can be characterised optically with a TIRF microscope. The waveguide is necessary to limit the exciting field to the enzyme at the bottom and thus reduce fluorescence from diffusing substrates (see online version for colours)
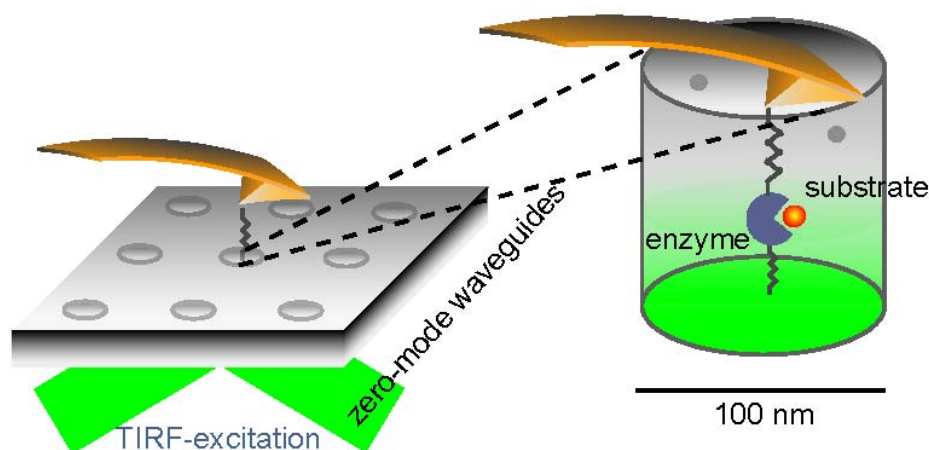
2   Zero-mode waveguides

2.1   Fabrication of zero-mode waveguides

For fabrication of ZMW, we used an FIB method described by Rigneault et al. [21]. Compared to the other two common ZMW fabrication methods, reactive ion etching [16] and eBeam-lithography [22], FIB milling is the least elaborate process. It consists of two basic steps: first blanks are fabricated by evaporating a thin aluminium film onto a glass substrate. Then nanometre-sized holes are milled into the aluminium film with an FIB.

We altered the first step and used negative tone optical lithography to produce blanks with orientation markers and wide glass windows. This was done to allow by-eye alignment of the AFM cantilever to designated ZMWs in the later experiments.

We cleaned conventional glass cover slips in consecutive ultrasonic bathes of acetone, isopropanol and double-distilled water (ddH$_2$O). Samples were then dried under a nitrogen stream and treated with oxygen plasma (Femto, Diener, Ebhausen, Germany) for 2 min at 100 W. To remove adsorbed water from the glass surface, substrates were heated up to 120°C for 2 min on a hot plate and cooled down under a dry steam of nitrogen just prior to photoresist coating. Negative tone photoresist (AZ5214E, Microchemicals, Ulm, Germany) was spun onto the substrates at 4000 rpm for 60 s with an accelerating ramp of 9 s followed by a prebake at 120°C for 60 s. Samples were exposed to UV-light (320 nm wavelength) for 35 s at 5.1 W/cm^2. During exposure, contact of a chromium mask with the substrate was achieved by a mask aligner (MA6, Suess Microtec, Garching, Germany). A post-exposure bake at 120°C for 120 s was followed by flood exposure of the whole surface for 105 s at the previously used wavelength and power. The exposed samples were developed in AZ726 (Microchemicals) for 40 s, dipped in consecutive stop and rinse baths of ddH$_2$O for 30 s each and then dried under a nitrogen stream. To remove undesired photoresist remains, samples were again treated with oxygen plasma for 60 s at 100 W power. A 110 nm thick aluminium film was evaporated in a thermal evaporator (306 Turbo, Edwards, Crawley, UK) with a rate of 0.1 nm/s at a pressure of 1.7×10^{-6} mbar. Lift-off was done in 40°C warm acetone. To support the lift-off process, a turbulent stream was created locally with handheld glass pipette. Samples were then cleaned by 30 s dips in isopropanol and ddH$_2$O followed by a rinse in ddH$_2$O and a final treatment with oxygen plasma for 120 s at 100 W.

We used a NVISION40 FIB (Zeiss, Oberkochen, Germany) to mill arrays of ZMWs into the designated metallic areas on the blanks. Array periodicity was 5 μm in the x-direction and the y-direction. The FIB aperture was set to 30 μm and the ion current was measured to be 10 pA at an acceleration bias of 30 kV. With these settings, milling doses for the ZMWs ranged from 120.000 to 200.000 μA/cm^2.

2.2   Characterisation of zero-mode waveguides

The challenge of the FIB-milling method comes from the manual focusing of the ion-beam, which requires optimisation and experience to fabricate reproducible ZMWs. Therefore, careful analysis of the fabricated structures is a prerequisite to successful experiments.

Due to the directionality of the milling process, the apertures' sidewalls converge towards the bottom of the hole rather than diverge. This makes the upper aperture diameter maximal and thus a sufficient criterion for an aperture being a ZMW. The depth of milling is set just below the glass interface to minimise negative effects of aluminium residues at the bottom of the aperture on the excitation and photophysical properties of the fluorophores as well as on the coupling efficiency for immobilisation.

ZMWs' opening diameters were analysed immediately after milling with the NVISION's SEM at an electron beam incidence angle of 54° (see Figure 3a). This allowed corrections of the FIB focus before milling further ZMWs on the same blank. AFM scans ensuring a sufficient depth was done later with a commercial AFM (MFP3D, Asylum Research, Santa Barbara, USA) operated in tapping mode in air. To correct for drift and sample tilt, a flattening algorithm was applied to the topography scans as the one shown in Figure 3b. To avoid not only slow scanning but also breakage of the cantilever, we chose a relatively robust cantilever (MSCT, Bruker, Camarillo, CA, USA). The SEM image of an MSCT tip in Figure 3c is a 90° side view of the tip and was made with a LEO-SEM (Zeiss). A comparison with the cantilever dimensions reveals that the cross-section in Figure 3b is rather a plot of the probe's shape than of the aperture. Nevertheless, opening diameter and minimal depth are still valid information from the scan.

Figure 3 (a) SEM image of a zero-mode waveguide. (b) Section through an AFM scan of a ZMW. The red line in the inserted scan marks the position of the section. (c) A SEM micrograph of the used cantilever's side view (see online version for colours)
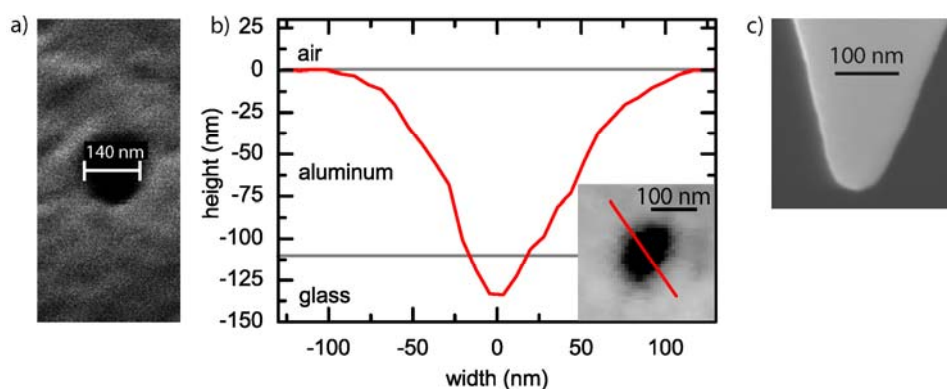
2.3 Corrosion of zero-mode waveguides

Working with ZMWs, we occasionally experienced degradation of samples due to corrosion. Although Korlach et al. [23] emphasised that passivation with polyvinylphosphonic acid prevents corrosion [23], corroded ZMWs have not yet been reported in the literature. In this section, we will thus present findings of corrosion and discuss possible mechanisms, reasons and precautions.

Aluminium is generally preferred over, for example, gold or silver as ZMW material. This is mainly due to its short skin depth and low-plasmonic coupling efficiency in the visible spectrum, where latter would increase the observation volume inside and above the ZMW by surface plasmon excitation. Another advantage of aluminium is its generally high-chemical stability and that it does not gradually oxidise and thus alter its

optical properties. Instead, aluminium forms a steady oxide layer of approximately 3 nm within seconds upon first contact to air and then remains unaltered for months if handled correctly [24]. However, when this passive layer is lost – even just locally – due to critical chemical conditions, impurities or physical stress, the underlying metal is subject to corrosion until an oxide layer reforms. For further details of the different corrosive processes see references [25, 26].

We found large areas (0.1–10 mm^2) of our aluminium surfaces corroded when stored in non-dry environments for days. We also witnessed corrosion upon abnormally high indentation with a cantilever. Most interestingly, however, we found signs for corrosion caused by the nanohole structures themselves.

Figure 4 shows a transmission image and an AFM-topography scan of a nanohole array milled for dose test purposes. Prior to the analysis, the sample had been incubated in 1x PBS buffer for 24 h. The original hole depth was approximately 60 nm into the 110 nm thick aluminium and original diameters had not exceeded 200 nm. One notices that some of the nanoapertures show perfectly circular corrosion patterns of arbitrary diameters ranging up to 4 μm, while other apertures remained unaltered. A striking feature best seen in the cross-section in Figure 4c is the thin rod that remained at the original hole position.

Figure 4   A transmitted light image (a) and an AFM topography scan (b) of the same nanohole array. The green grid (5 μm periodicity) was drawn to guide the eye. The nanoholes had an original depth of approximately 60 nm into the 110 nm thick aluminium film. The green arrows point out a pillar remaining at the original position of a corroded hole. The actual depth of the uncorroded nanohole (blue arrow) is not resolved in this scan (see online version for colours)
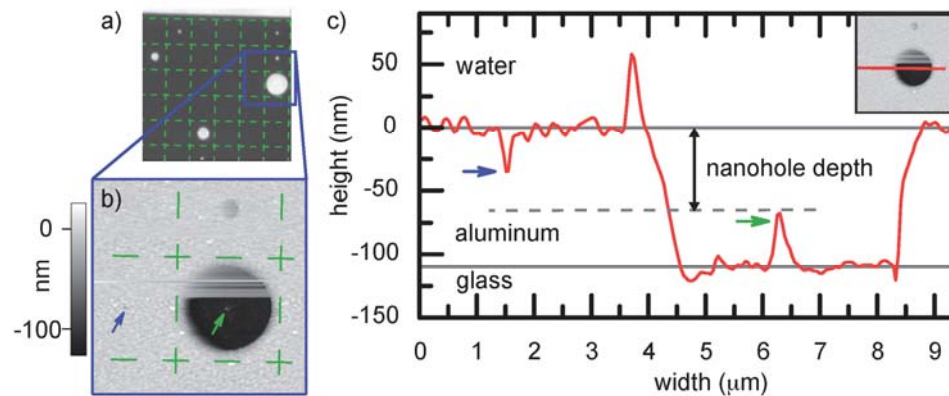
We interpret this rod as corrosion resistant, aluminium remains contaminated with FIB gallium ions. Contaminations are a known side effect of FIB milling [27]. These gallium remains are also a possible cause for an insufficient formation of the apertures' oxide layer that would then allow corrosion to start.

Another explanation for corrosion nucleation or corrosion enhancement in nanoapertures is related to their geometry: their confined volume limits diffusion and thus enhances autocatalytic pathways including the accumulation of chloride ions and the prevention of surface passivation by oxygen. This phenomenon is known, for example, micro cracks or other confined microstructures in material science as crevice corrosion

[25, 26]. This interpretation of our corrosion findings is especially striking, since it is an intrinsic property of the apertures and independent of our FIB-milling method.

We learned to drastically reduce corrosion by storing ZMW samples under argon and by avoiding buffers with chloride ions where possible.

3   Combined force and fluorescence spectroscopy of titin kinase

3.1   Experiment

Combined force and fluorescence spectroscopy was performed on a homebuilt AFM-TIRF-hybrid instrument described by Gumpp et al. [9]. However, we used a different 532 nm laser (Cobolt Samba, Cobolt, Stockholm, Sweden), a lower magnification oil objective (CFI Apochromat TIRF 60× oil, N.A. 1.49, Nikon, Tokyo, Japan) and another EMCCD-camera (iXon + 860, Andor, Belfast, Northern Ireland). The AFM part of the instrument did not differ from the one described in the publication.

To synchronise both units of the instrument, an additional source code was implemented in the AFM software. Thus, at the start of a force-pulling event, the AFM-controller triggered the EMCCD-camera via the camera's external trigger.

Expression and purification of the TK protein construct A168M2 (867 amino acids, from position 24422–25288 in human cardiac N2-B titin, accession No. NP 003310.3) is described in the supporting material of Puchner et al. [12]. For the actual experiments combining force-activation and fluorescence spectroscopy, 0.5 μM TK was incubated in HEPES buffer (40 mM, pH 7.2, 2 mM $MgCl_2$) on untreated ZMWs for 20 min.

The approximate diameter of the used apertures was 150 nm. TK that did not adsorb to the substrate was washed away by buffer exchange. For the measurement, HEPES buffer containing 1 μM ATP was used. The ATP was labelled with a Cy3 dye at the gamma phosphate and is commercially available from Jena Bioscience (Jena, Germany).

To allow access to most of the ZMW's bottom, we used a high aspect ratio cantilever (Biolever Mini, Olympus, BL-AC40TS), which also showed less fluorescence background signal from inelastic scattering due to its silicon tip. In SEM images (not shown), we measured the cantilever's width to be smaller than 50 nm at a distance of 110 nm away from its tip thus allowing to probe the inner 100 nm wide disc of a 150 nm diameter hole. To avoid large area AFM scans resulting in a TK clogged cantilever, we did a broad alignment of the cantilever's shadow (light source was a handheld flashlight by MagLite, USA) and the ZMWs (visible from diffusing of labelled ATP in TIRF configuration). Following this alignment procedure, we were able to localise individual ZMWs in 1 × 1 μm topography scans. We then started our force-pulling routines with the cantilever localised in the ZMW's centre. After 100 force-pulling events another 1 × 1 μm topography scan ensured that our cantilever's picking position had not moved out of the ZMW despite thermal drift.

A force-pulling event started with an approach at 3 μm/s velocity. Pulling velocities were varied: during the first 75 nm of retraction, a reduced pulling velocity of 200 nm/s was applied in order to widen the time window in which a substrate could bind. The remaining pull was done with a speed of 1 μm/s.

For the fluorescence time traces shown in Figures 5 and 6, the mean signal of a 3 × 3 pixel square containing the ZMW's centre was calculated and plotted over time.

Figure 5   Fluorescence intensity of Cy3-labelled ATP molecules (0.5 μM) diffusing in and out of a ZMW. The average dwell time is less than the camera's time resolution of 1 ms (see online version for colours)
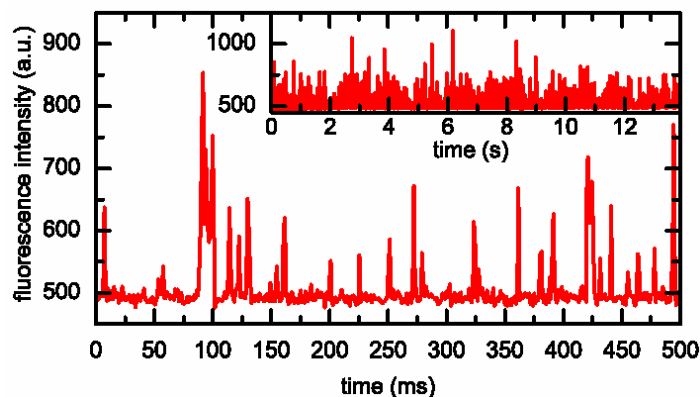
Figure 6   Two force-pulling curves from the bottom of a ZMW show the characteristic unfolding pattern of titin kinase (upper curves). The pulling speed was switched from 200 to 1000 nm/s at approximately 75 nm above the surface (grey line). The fluorescence intensity signal (lower curves) shows background only in the left case and a possible ATP binding event around 0.83 s (marked with a star) in the right case (see online version for colours)
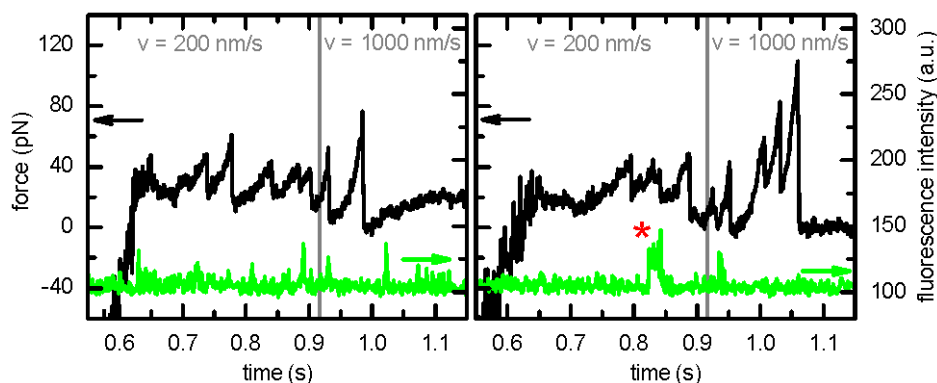
3.2   Results and discussion

To test sufficient optical confinement and thus ZMW characteristics of our nanoapertures, we first recorded fluorescence from diffusing labelled ATP in the absence of TK.

A typical fluorescence time trace is shown in Figure 5. The separated spikes of varying height and dwell times below the camera's time resolution of 1 ms are characteristic for concentrations below single-molecule occupation [16]. Spike frequency is in the order of the theoretical occupancy of 0.015 molecules given by equation (1) when assuming an illumination depth of 20 nm and 150 nm ZMW diameters. An autocorrelation analysis (data not shown) did not exhibit plateaus within our time resolution. These results verify strong optical confinement and thus ZMW character.

Compared to these initial experiments, we chose one magnitude less laser power and a twofold ATP concentration for the actual force-activation experiments to minimise dye bleaching and increase substrate-binding probabilities, respectively.

Figure 6 shows force and fluorescence intensity data recorded during force-pulling events in ZMWs. Both force curves show the characteristic unfolding pattern of TK with its attached Ig-domains. The two corresponding fluorescence traces show spikes below the resolution limit that we denote as diffusing ATP. Additionally the right time trace features a distinct fluorescence plateau (marked with a star). In agreement with reference [14], the plateau appears just after unfolding of the second barrier and its length of approximately 30 ms is too long to be explained with a non-bound merely diffusing ATP molecule (Figure 5).

This distance correlation and the lacking of similar fluorescence signatures in other force curves recorded in the same experiment suggest that the recorded data shown in Figure 6b is optical evidence of single ATP molecule binding to a TK upon force-activation.

Stronger evidence has to be given by statistics. However, our described experiment is yet far from a high-throughput method. We only found eight clear TK unfolding signatures in a total of 700 recorded force curves, distributed over ten ZMWs. This yield of 1% is comparable to other unspecific force spectroscopy measurements with that TK construct. Since our protocol cannot be completely automated so far and its trace acquisition rate is much lower, a long-term measurement over several days is not feasible. A straight forward method to enhance this yield is the use of a specific immobilisation procedure or – more sophisticated – the employment of SMC&P. Latter can be used to pick up proteins in small but very dense protein depots and probe them upon anchoring in a ZMW. Another factor limiting our statistics is the collection of protein during localisation scans that eventually leads to clogging of the cantilever. An optical alignment procedure using super-resolution techniques to localise and non-invasively align cantilever and ZMW could make AFM scans obsolete.

4 Conclusion

For the optical investigation of substrate binding to mechanoactive enzymes, physiologically high equilibrium concentrations are not only scientifically desirable but also an experimental requirement. As discussed above, this intrinsic demand comes from signal-to-background limitations as well as the short time window between the activation of a force-activated enzyme and its rupture under the tension caused by the activation. So far background fluorescence going along with these high substrate concentrations prevented the optical observation of single-binding events in such experiments.

In the study presented here, we showed how ZMWs can be used to overcome these limitations. We characterised the necessary fabrication methods and designs as well as the chemical environment necessary for such an experiment. Meeting these conditions, we were able to conduct the first experiment that optically observed the binding of a single substrate to an enzyme force-activated at the bottom of a ZMW.

With this first proof of principle, we believe that the use of ZMWs will now allow the application of the powerful techniques of fluorescence microscopy in their whole bandwidth and thus open up unprecedented characterisation possibilities for force-activated enzymes.

In a more general view, the proven possibility to mechanically access and manipulate molecules in ZMWs widens the range of applications for ZMWs even further. For example, this opens up the possibility to use SMC&P in ZMWs. Applied to ZMWs, SMC&P could be used to selectively immobilise anchors or enzymes at desired positions, like hotspots within the nanoapertures.

Acknowledgements

References

1   Neher, E. and Sakmann, B. (1976) 'Single-channel currents recorded from membrane of denervated frog muscle fibres', *Nature*, Vol. 260, No. 5554, pp.799–802.

2   Tinnefeld, P. and Sauer, M. (2005) 'Branching out of single-molecule fluorescence spectroscopy: challenges for chemistry and influence on biology', *Angewandte Chemie International Edition*, Vol. 44, No. 18, pp.2642–2671.

3   Florin, E., Moy, V. and Gaub, H.E. (1994) 'Adhesion forces between individual ligand-receptor pairs', *Science*, Vol. 264, No. 5157, pp.415–417.

4   Nishizaka, T., Miyata, H., Yoshikawa, H., Ishiwata, S. and Kinosita Jr., K. (1995) 'Unbinding force of a single motor molecule of muscle measured using optical tweezers', *Nature*, Vol. 377, No. 6546, pp.251–254.

5   Rief, M., Gautel, M., Oesterhelt, F., Fernandez, J.M. and Gaub, H.E. (1997) 'Reversible unfolding of individual titin immunoglobulin domains by AFM', *Science*, Vol. 276, No. 5315, pp.1109–1112.

6   Clausen-Schaumann, H., Rief, M., Tolksdorf, C. and Gaub, H.E. (2000) 'Mechanical stability of single DNA molecules', *Biophysical Journal*, Vol. 78, No. 4, pp.1997–2007.

7   Woodside, M.T., Anthony, P.C., Behnke-Parks, W.M., Larizadeh, K., Herschlag, D. and Block, S.M. (2006) 'Direct measurement of the full, sequence-dependent folding landscape of a nucleic acid', *Science*, Vol. 314, No. 5801, pp.1001–1004.

8   Kufer, S.K., Puchner, E.M., Gumpp, H., Liedl, T. and Gaub, H.E. (2008) 'Single-molecule cut-and-paste surface assembly', *Science*, Vol. 319, No. 5863, pp.594–596.

9   Gumpp, H., Stahl, S.W., Strackharn, M., Puchner, E.M. and Gaub, H.E. (2009) 'Ultrastable combined atomic force and total internal fluorescence microscope', *Review of Scientific Instruments*, Vol. 80, No. 6, pp.063704–063705.

10   Gumpp, H., Puchner, E.M., Zimmermann, J.L., Gerland, U., Gaub, H.E. and Blank, K. (2009) 'Triggering enzymatic activity with force', *Nano Letters*, Vol. 9, No. 9, pp.3290–3295.

11   Strackharn, M., Stahl, S.W., Puchner, E.M. and Gaub, H.E. (2012) 'Functional assembly of aptamer binding sites by single-molecule cut-and-paste', *Nano Letters*, Vol. 12, No. 5, pp.2425–2428.

12   Puchner, E.M., Alexandrovich, A., Kho, A.L., Hensen, U., Schäfer, L.V., Brandmeier, B., Gräter, F., Grubmüller, H., Gaub, H.E. and Gautel, M. (2008) 'Mechanoenzymatics of titin kinase', *Proceedings of the National Academy of Sciences*, Vol. 105, No. 36, pp.13385.

13 Stahl, S.W., Puchner, E.M., Alexandrovich, A., Gautel, M. and Gaub, H.E. (2011) 'A conditional gating mechanism assures the integrity of the molecular force-sensor titin kinase', *Biophysical Journal*, Vol. 101, No. 8, pp.1978–1986.

14 Puchner, E.M. and Gaub, H.E. (2010) 'Exploring the conformation-regulated function of titin kinase by mechanical pump and probe experiments with single molecules', *Angewandte Chemie International Edition*, Vol. 49, No. 6, pp.1147–1150.

15 Samiee, K., Foquet, M., Guo, L., Cox, E. and Craighead, H. (2005) 'Lambda-repressor oligomerization kinetics at high concentrations using fluorescence correlation spectroscopy in zero-mode waveguides', *Biophysical Journal*, Vol. 88, No. 3, pp.2145–2153.

16 Levene, M.J., Korlach, J., Turner, S.W., Foquet, M., Craighead, H.G. and Webb, W.W. (2003) 'Zero-mode waveguides for single-molecule analysis at high concentrations', *Science*, Vol. 299, No. 5607, pp.682–686.

17 Miyake, T., Tanii, T., Sonobe, H., Akahori, R., Shimamoto, N., Ueno, T., Funatsu, T. and Ohdomari, I. (2008) 'Real-time imaging of single-molecule fluorescence with a zero-mode waveguide for the analysis of protein− protein interaction', *Analytical Chemistry*, Vol. 80, No. 15, pp.6018–6022.

18 Samiee, K.T., Moran-Mirabal, J.M., Cheung, Y.K. and Craighead, H.G. (2006) 'Zero mode waveguides for single-molecule spectroscopy on lipid membranes', *Biophysical Journal*, Vol. 90, No. 9, pp.3288–3299.

19 Moran-Mirabal, J.M., Torres, A.J., Samiee, K.T., Baird, B.A. and Craighead, H.G. (2007) 'Cell investigation of nanostructures: zero-mode waveguides for plasma membrane studies with single molecule resolution', *Nanotechnology*, Vol. 18, No. 19, p.195101.

20 Eid, J., Fehr, A., Gray, J., Luong, K., Lyle, J. and Turner, S. (2009) 'Real-time DNA sequencing from single polymerase molecules', *Science*, Vol. 323, No. 5910, pp.133–138.

21 Rigneault, H., Capoulade, J., Dintinger, J., Wenger, J., Bonod, N., Popov, E., Ebbesen, T. and Lenne, P-F. (2005) 'Enhancement of single-molecule fluorescence detection in subwavelength apertures', *Physical Review Letters*, Vol. 95, No. 11, pp.117401.

22 Foquet, M., Samiee, K.T., Kong, X., Chauduri, B.P., Lundquist, P.M., Turner, S.W., Freudenthal, J. and Roitman, D.B. (2008) 'Improved fabrication of zero-mode waveguides for single-molecule detection', *Journal of Applied Physics*, Vol. 103, No. 3, p.034301.

23 Korlach, J., Marks, P.J., Cicero, R.L., Gray, J.J., Murphy, D.L., Roitman, D.B., Pham, T.T., Otto, G.A., Foquet, M. and Turner, S.W. (2008) 'Selective aluminum passivation for targeted immobilization of single DNA polymerase molecules in zero-mode waveguide nanostructures', *Proceedings of National Academy of Science USA*, Vol. 105, No. 4, pp.1176–1181.

24 Zhu, P. and Craighead, H.G. (2012) 'Zero-mode waveguides for single-molecule analysis', *Annual Review of Biophysics*, Vol. 41, No. 1, pp.269–293.

25 Szklarska-Smialowska, Z. (1999) 'Pitting corrosion of aluminum', *Corrosion Science*, Vol. 41, No. 9, pp.1743–1767.

26 Vargel, C. (2004) *Corrosion of Aluminium*, Elsevier, Amsterdam.

27 Han, G., Weber, D., Neubrech, F., Yamada, I., Mitome, M., Bando, Y., Pucci, A. and Nagao, T. (2011) 'Infrared spectroscopic and electron microscopic characterization of gold nanogap structure fabricated by focused ion beam', *Nanotechnology*, Vol. 22, No. 27, p.275202.